International Journal of GEOMATE, Nov., 2019 Vol.17, Issue 63, pp. 297 - 306
ISSN: 2186-2982 (P), 2186-2990 (O), Japan, DOI: https://doi.org/10.21660/2019.63.25640
Geotechnique, Construction Materials and Environment

APPLICATION OF DIGITAL IMAGE TECHNOLOGY FOR DETERMINING GEOMETRY, STRATIGRAPHY, AND POSITION OF CRACKS INSIDE EARTH SLOPE

* Dewi Amalia [1], Indrasurya Budisatria Mochtar [2] and Noor Endah Mochtar [3]

[1] Civil Engineering Department, Politeknik Negeri Bandung, Indonesia; [1,2,3] Civil Engineering Department, Institut Teknologi Sepuluh Nopember (ITS), Indonesia

*Corresponding Author, Received: 11 April 2019, Revised: 29 April 2019, Accepted: 25 May 2019

ABSTRACT: In the concept of cracked soils, one of the important factors for determining slope stability is the position of cracks. The position of cracks has been successfully obtained by other study using geoelectric testing. The geoelectric data produces several colors that describe the conditions of the slope geometry, soil stratigraphy, and the position of the cracks inside the slope. In order to improve the accuracy of reading geoelectric data for slope stability analysis, a digital image processing technique is proposed here. This digital image technology is applied by means of an auxiliary program based on the graphical user interface (GUI) that exists inside the MATLAB m-files and utilizing the option of RGB (Red, Green, Blue) color formats. With this technique, geoelectric data retrieval will take place automatically, thus it can be directly used as input for the slope stability analysis program to determine the value of the slope safety factor. The image processing technique in this study is based on using a straight-line equation to detect slope geometry, soil stratigraphy, and the position of cracks on slopes based on the geoelectric data. The simulation results in this study provide sufficiently accurate values of geoelectric data retrieval, which is to reach 5.78 cm/pixel. The larger the pixel size of the processed slope image, the higher the accuracy of the program outcomes. The results of this study will be later used for input in the new slope stability analysis based on cracked soil approaches utilizing digital image technology.

Keywords: Tomographic Resistivity (TR), Induced Polarization (IP), Digital image processing, Earth slope

1. INTRODUCTION

A suggested a new method of cracked soil approaches for slope stability analysis had been suggested by Mochtar, et. al. [1-5]. Afterward, Alexander, Mochtar, and Utama [6-7] had suggested a new method of determining cracks inside the soil slope by using the geoelectric method, and the results were obtained using digital image technology. However, other studies are still needed, which mainly: (1) to connect the results of geoelectric measurement into the slope stability analysis and (2) to establish the new slope stability analysis using the cracked soil concept utilizing the digital image technology. This paper is to answer the first study, while the second study will be described in another paper in the near future.

Geoelectric is a method of geophysical exploration to investigate sub-surface conditions by measuring the electrical properties of soil or rocks. The applications of geoelectric have been widely used in various fields of science. Some of the examples for the application of geoelectric on civil engineering field are to find out the soil and rock stratigraphy [8], groundwater position [9], position of the aquifer [10], soil and rock permeability and porosity [11], location of the bedrock [10], and to determine dimension and depth of foundation and other buried structures [12].

Geoelectric data can be applied directly, for example, to determine the position of the aquifer in the soil. However, when it comes to the need for further analysis such as the analysis of slope stability, the use of geoelectric raw data is seen as less practical. For example, to determine the slope geometry, the user must plot the data manually one by one; thus, the user must transfer the results of geoelectric data to the slope stability analysis program [6-7]. In addition, the results obtained by the manual method are deemed inaccurate and require a long time to transfer the raw geoelectric data to the slope stability analysis software. Therefore, innovation to improve the accuracy and the speed of the process of transferring geoelectric data to the slope stability analysis software is needed, namely using the digital image processing technology.

In its development, image processing can be used to distinguish types of products because this technology can analyze products based on differences in color intensity. The ability of image processing technology was applied and developed to interpret the geoelectric test results on an earth slope so that the geometry, soil stratigraphy and

crack position inside the slope can be produced.

Output data from geoelectric survey results are processed using digital image technology in the form of tomographic resistivity and induced polarization data. The tomographic resistivity, TR, values are obtained from measuring the potential differences, current strengths, and resistance at the geoelectric survey. The induced polarization, IP, values are obtained based on the time duration the electric current can still remain in the soil after the geoelectric survey is turned off. Examples of the results of geoelectric surveys can be seen in Figures 1 and 2.

In the following Figures 1 and 2, two examples of geoelectric data from Alexsander et.al. [6] are given in the form of digital image technology. The values of tomographic resistivity, TR, in Figure 1 provide information that the blue color areas, in general, should indicate higher water concentration, while the red color areas indicate a lower water concentration, according to the color scale shown at the bottom of the image. Induced polarization, IP, values in Figure 2 inform that the red color areas contain some cracks, and the blue color areas are still quite solid (not cracked). This digital data will be further processed using a method to be described later in this paper.

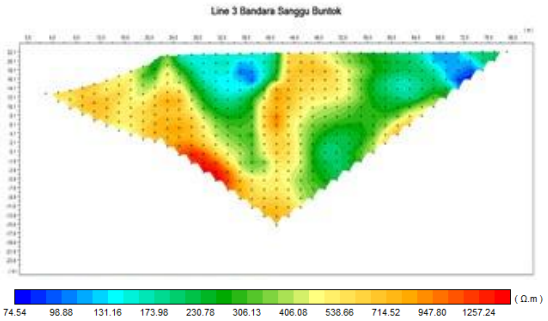

Fig.1 Two-dimensional Tomographic Resistivity, TR Results of geoelectric measurement [6]

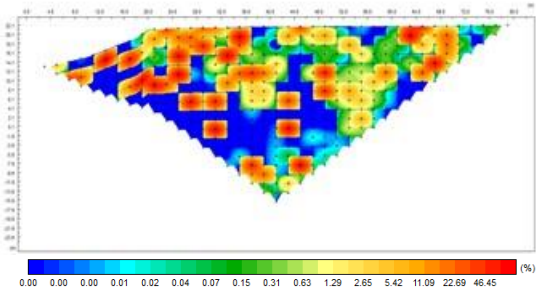

'Fig.2 Two-dimensional Induced Polarization, IP, Results of geoelectric measurement [6]

This research is meant to give contribution to the state-of-the-art of the development and application in the field in computational science combined with geotechnical and geophysical science. This research is also aimed to support the development of the concept of cracked soil [1-7, 13].

The output from this research is manifested in a program based on the graphical user interface (GUI) using MATLAB m-file. This digital image processing technique facility is not yet available in the application or commercial program of slope stability analysis. It is expected that digital image processing techniques in this study provide a breakthrough in the geotechnical field, especially in analyzing slope stability.

2. METHODOLOGY

The image processing technique used in this study is image processing techniques with RGB (Red, Green, and Blue) color spaces. The geoelectric image was converted into an RGB matrix where the size of the matrix will be the same as the pixel size in the image. Afterward, the matrix was further processed so that the slope geometry, soil layer, and areas that contain some cracks can all be modeled separately. The results can be carried out in three models, namely:

a. Model-1, which is done to determine the slope geometry. The processed data are obtained from the tomographic resistivity, TR, data.
b. Model-2, which is done to determine the soil stratigraphy. The processed data are also obtained from the TR data.
c. Model-3, which is done to determine the position of the cracks. The processed data obtained from the TR and IP data.

The results from the above three models will be used to speed up the processes of inputting data of the slope geometry, soil stratigraphy, and positions of cracks. This process of using digital image technology is also proven to be more accurate than the process of inputting data manually.

The above method, however, up to this stage is still not yet satisfactory, because the techniques developed in this process can still not be directly applied on the existing programs of slope stability analysis (i.e. GEOSTUDIO, XSTABL, or PLAXIS). For this purpose, the authors are currently preparing a new program of slope stability analysis that will directly apply all the assumptions of cracked soil phenomena, while using the new techniques of inputting the digital image technology directly into the program. This new program, however, will be described in other paper in the near future.

3. RESULTS AND DISCUSSIONS

In processing digital images, there are several color space formats such as RGB (Red, Green, Blue), CMYK (Cyan, Magenta, Yellow Key), HSV (Hue, Saturation, Value), HSL (Hue, Saturation, Lightness), HSB (Hue, Saturation, Brightness), and YUV (Y is the lumen component or brightness, U is the chromatic component of blue lighting, and V is the chromatic component of red lighting) which can be simply understood as the basic color that forms any color [14]. The image processing technique used in this study is of that of RGB (Red, Green, Blue) color space. Figure 3 is an example of an illustration of 8 × 8 pixels.

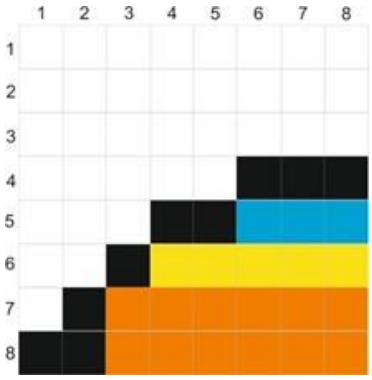

Fig.3. Example illustration of an image having 8 × 8 pixels size

An image is composed of several 8 × 8 pixels of colors shown in Figure 3. Then the image is interpreted into an RGB color space, to produce 3 red, green, and blue matrices, which are the color codes that make up the image. To simplify the above concept, an example is given of color with a size of 1 × 1 pixel as follows:

White : Red = [255], Green = [255], Blue = [255]
Black : Red = [0], Green = [0], Blue = [0]
Light Blue: Red = [0], Green = [175], Blue = [18].

From the example in Figure 3, color in RGB color space is composed of 3 basic color codes of red, green, and blue; and the size of the matrix is the same as the pixel size of the image. Greater color code values in red, green, and blue will make the colors tend to fade and lead to the color white, and vice versa. Whereas, smaller color code value will make the colors tend to be darker and lead to the color of black. If the image in Figure 3 with the size of 8 × 8 pixels is interpreted in an RGB color space, three red, green, and blue matrices are obtained with 8 × 8 matrix sizes as follows:

$$\boldsymbol{Red} = \begin{bmatrix} 255 & 255 & 255 & 255 & 255 & 255 & 255 & 255 \\ 255 & 255 & 255 & 255 & 255 & 255 & 255 & 255 \\ 255 & 255 & 255 & 255 & 255 & 255 & 255 & 255 \\ 255 & 255 & 255 & 255 & 255 & 0 & 0 & 0 \\ 255 & 255 & 255 & 0 & 0 & 0 & 0 & 0 \\ 255 & 255 & 0 & 255 & 255 & 255 & 255 & 255 \\ 255 & 0 & 245 & 245 & 245 & 245 & 245 & 245 \\ 0 & 0 & 245 & 245 & 245 & 245 & 245 & 245 \end{bmatrix} \quad (1)$$

$$\boldsymbol{Green} = \begin{bmatrix} 255 & 255 & 255 & 255 & 255 & 255 & 255 & 255 \\ 255 & 255 & 255 & 255 & 255 & 255 & 255 & 255 \\ 255 & 255 & 255 & 255 & 255 & 255 & 255 & 255 \\ 255 & 255 & 255 & 255 & 255 & 0 & 0 & 0 \\ 255 & 255 & 255 & 0 & 0 & 175 & 175 & 175 \\ 255 & 255 & 0 & 242 & 242 & 242 & 242 & 242 \\ 255 & 0 & 134 & 134 & 134 & 134 & 134 & 134 \\ 0 & 0 & 134 & 134 & 134 & 134 & 134 & 134 \end{bmatrix} \quad (2)$$

$$\boldsymbol{Blue} = \begin{bmatrix} 255 & 255 & 255 & 255 & 255 & 255 & 255 & 255 \\ 255 & 255 & 255 & 255 & 255 & 255 & 255 & 255 \\ 255 & 255 & 255 & 255 & 255 & 255 & 255 & 255 \\ 255 & 255 & 255 & 255 & 255 & 0 & 0 & 0 \\ 255 & 255 & 255 & 18 & 18 & 18 & 18 & 18 \\ 255 & 255 & 0 & 255 & 255 & 255 & 255 & 255 \\ 255 & 0 & 52 & 52 & 52 & 52 & 52 & 52 \\ 0 & 0 & 52 & 52 & 52 & 52 & 52 & 52 \end{bmatrix} \quad (3)$$

The basis of the image processing techniques above will then be used to process and interpret the slope geoelectric test data and the results are described in the following sections.

3.1 Model 1, Determination of Slope Geometry

Slope geometry modeling can be formed from several points (x_n, y_n), and then these points are connected by straight lines as shown in Figure 4. From the modeling, a simple matrix equation model is obtained and shown in Equations (4) and (5).

$$x_n = [x_1\ x_2\ x_3\ x_4\ x_5\ x_6\ x_7\ x_8\ x_9\ x_{10} \ldots\ x_n] \quad (4)$$

$$y_n = [y_1\ y_2\ y_3\ y_4\ y_5\ y_6\ y_7\ y_8\ y_9\ y_{10} \ldots\ y_n] \quad (5)$$

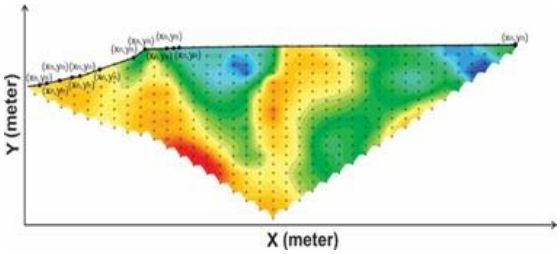

Fig.4 Model results of geoelectric test data and data input for image processing technique

The stages of geoelectric data procession using digital image technology to obtain slope geometry can be arranged as a flow chart in Figure 5.

The above stages of digital image processing in Figure 5 can be explained as follows:

1. Inputting images of the geoelectric test data. At this stage, the length and height of the geoelectric image are scaled to the actual size of the slope in the field.
2. Reading pixel data from the geoelectric test data image in RGB color space. If the example in Figure 3 is used, the matrix obtained is those of Equations (1), (2), and (3).
3. Converting three red, green, and blue matrices into a greyscale matrix, as in Equations 6.

$$[Grey] = 0.2989 .\times [Red] + 0.5870 .\times [Green] + 0.1140 .\times [Blue] \quad [15] \quad (6)$$

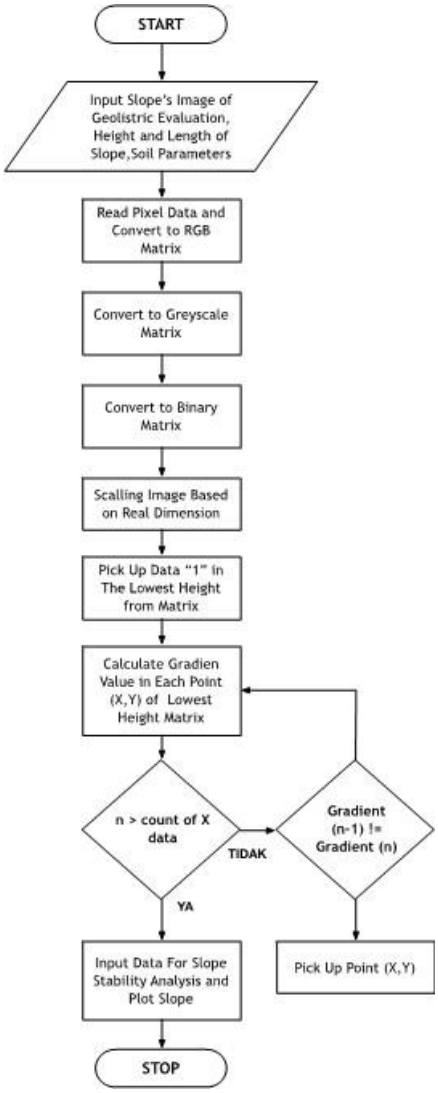

Fig.5 Flowchart to obtain slope geometry data from geoelectric test results

The results of Equation (6) can be applied into Equations (1), (2), and (3) to produce a gray matrix as shown in Equation (7). From the matrix above, a comparison of changes will be obtained as shown in Figure 6.

$$\begin{bmatrix} 254 & 254 & 254 & 254 & 254 & 254 & 254 & 254 \\ 254 & 254 & 254 & 254 & 254 & 254 & 254 & 254 \\ 254 & 254 & 254 & 254 & 254 & 254 & 254 & 254 \\ 254 & 254 & 254 & 254 & 254 & 0 & 0 & 0 \\ 254 & 254 & 254 & 0 & 0 & 104 & 104 & 104 \\ 254 & 254 & 0 & 247 & 247 & 247 & 247 & 247 \\ 254 & 0 & 160 & 160 & 160 & 160 & 160 & 160 \\ 0 & 0 & 160 & 160 & 160 & 160 & 160 & 160 \end{bmatrix} \quad (7)$$

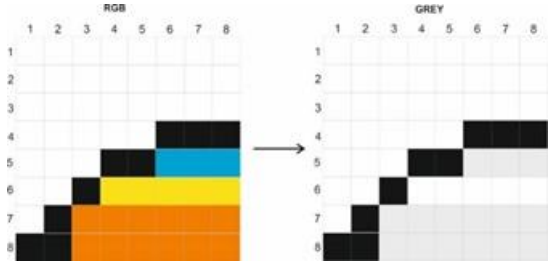

Fig.6 Comparison of RGB and GRAY images

4. The conversion of grey matrix into the form of binary matrices is done via the following equations:

   if *grey* (n,n) < 1, then *grey* (n,n) = 0 (8)
   if *grey* (n,n) ≥ 1, then *grey* (n,n) = 1 (9)

   By using Equations (8) and (9) the binary matrix shown in Equation (10) is produced.

$$\boldsymbol{Binary} = \begin{bmatrix} 1 & 1 & 1 & 1 & 1 & 1 & 1 & 1 \\ 1 & 1 & 1 & 1 & 1 & 1 & 1 & 1 \\ 1 & 1 & 1 & 1 & 1 & 1 & 1 & 1 \\ 1 & 1 & 1 & 1 & 1 & 0 & 0 & 0 \\ 1 & 1 & 1 & 0 & 0 & 1 & 1 & 1 \\ 1 & 1 & 0 & 1 & 1 & 1 & 1 & 1 \\ 1 & 0 & 1 & 1 & 1 & 1 & 1 & 1 \\ 0 & 0 & 1 & 1 & 1 & 1 & 1 & 1 \end{bmatrix} \quad (10)$$

   The results of the final comparison of images from grey to binary are shown in Figure 7.

5. Multiplying the pixel size of the image with the real length and height of the slope will produce a pixel size that represents the actual size. In this example, if the actual size is 80 × 80 m, then the size of each pixel is 10 meters.

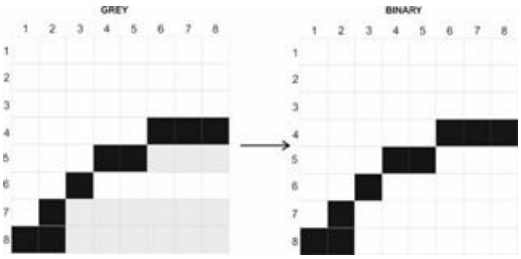

Fig.7 Comparison of grey and binary images

6. Retrieving data position *(x,y)* from the value '0' on the binary matrix in each column and selecting the value '0' with the top position, or with the position of the value *(y)* as the smallest in each column. For more details, it can be visualized in the Equation (11) for the selected value of '0' marked in green.

$$\boldsymbol{Binary} = \begin{bmatrix} 1 & 1 & 1 & 1 & 1 & 1 & 1 & 1 \\ 1 & 1 & 1 & 1 & 1 & 1 & 1 & 1 \\ 1 & 1 & 1 & 1 & 1 & 1 & 1 & 1 \\ 1 & 1 & 1 & 1 & 1 & 0 & 0 & 0 \\ 1 & 1 & 1 & 0 & 0 & 1 & 1 & 1 \\ 1 & 1 & 0 & 1 & 1 & 1 & 1 & 1 \\ 1 & 0 & 1 & 1 & 1 & 1 & 1 & 1 \\ 0 & 0 & 1 & 1 & 1 & 1 & 1 & 1 \end{bmatrix} \quad (11)$$

From Equation (11) above, the selected value of '0' is shown. The next step is to take position data *(x, y)* from the value of '0' selected in the binary matrix. The results of the selected list of values of '0' are shown in the following matrix equation:

$$\boldsymbol{x} = [1 \quad 2 \quad 3 \quad 4 \quad 5 \quad 6 \quad 7 \quad 8] \quad (12)$$

$$\boldsymbol{y} = [8 \quad 7 \quad 6 \quad 5 \quad 5 \quad 4 \quad 4 \quad 4] \quad (13)$$

Then, to conform with the *x – y* curve rules, matrix x and y needs to be converted into the following equations:

$$x_{new} = x(1, n) - 1 \quad (14)$$

$$y_{new} = \text{max pixel} - y(1,n) \quad (15)$$

where:

n = member of the x or y of the order - n

The matrix x_{new} and y_{new} are as follows:

$$\boldsymbol{x\,new} = [0 \quad 1 \quad 2 \quad 3 \quad 4 \quad 5 \quad 6 \quad 7] \quad (16)$$

$$\boldsymbol{y\,new} = [0 \quad 1 \quad 2 \quad 3 \quad 3 \quad 4 \quad 4 \quad 4] \quad (17)$$

7. Calculation of gradient values from each position shown in the matrix Equations (16) and (17) using the following equation:

$$\boldsymbol{m} = \frac{y2 - y1}{x2 - x1} \quad (18)$$

From Equation (18) the gradient results are shown as shown in Equation (19):

$$\boldsymbol{m} = [1 \quad 1 \quad 1 \quad 0 \quad 1 \quad 0 \quad 0] \quad (19)$$

8. Selection of positions shown in Equation (16) and (17) based on matrix values in Equation (19) with the following conditions:

(x_{chosen}, y_{chosen}) if $m(n) \neq m(n+1)$ (20)

From Equations 19 and 20, the m_{chosen}, x_{chosen} dan y_{chosen} matrices are obtained, which are the click points (at this stage there is no need for all points *(x, y)* to be entered). The selection results are shown in the following matrix equations:

$$\boldsymbol{m\,chosen} = [1 \quad 1 \quad 0 \quad 1] \quad (21)$$

$$\boldsymbol{x\,chosen} = [0 \quad 3 \quad 4 \quad 5] \quad (22)$$

$$\boldsymbol{y\,chosen} = [0 \quad 3 \quad 3 \quad 4] \quad (23)$$

9. The final stage is to add the position of the last point of the matrix in Equations (22) and (23) namely $x_{last} = 7$ and $y = 4$ on the equations x_{chosen} and y_{chosen} thus the new matrix is selected and the new one is chosen as follows:

$$\boldsymbol{x\,chosen\,new} = [0 \quad 3 \quad 4 \quad 5 \quad 7] \quad (24)$$

$$\boldsymbol{y\,chosen\,new} = [0 \quad 3 \quad 3 \quad 4 \quad 4] \quad (25)$$

After obtaining $x_{chosen\ new}$ and $y_{chosen\ new}$, then plotting is done according to Equations (24) and (25). The plotting results can be seen in Figure 8.

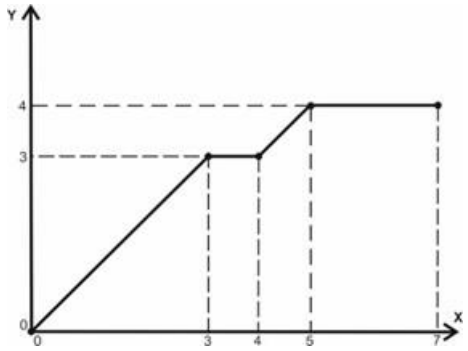

Fig.8 Curve plotting of the ($x_{chosen\ new}$, $y_{chosen\ new}$)

From all the stages described above, the slope geometry data are automatically obtained from the geoelectric results and the slope geometry data in the form of curves and (x, y) matrices are also produced so that the slope stability analysis program can be directly executed.

3.2 Model 2, Determination of Soil Stratigraphy

For the determination of soil stratigraphy, the Tomographic Resistivity, TR, data are needed as seen in Figure 9. In Figure 9, several lines and a number on click points are drawn as the borders of the green and yellow areas. The click points are what will be used to detect differences in soil parameters (soil layers). These results will be compared to soil data from soil boring tests before being simulated in the soil stability program.

Equations (4) and (5) also represent the modeling of soil layers in Figure (6) (written with (x_{ln}, y_{ln})). The results of the simple matrix equation model in Figure 9 are shown in Equations (26) and (27).

$$x_{ln} = [x_1\ x_2\ x_3\ x_4\ x_5\ x_6\ x_7\ x_8\ x_9 \ldots\ x_{ln}] \quad (26)$$

$$y_{ln} = [y_1\ y_2\ y_3\ y_4\ y_5\ y_6\ y_7\ y_8\ y_9 \ldots\ y_{ln}] \quad (27)$$

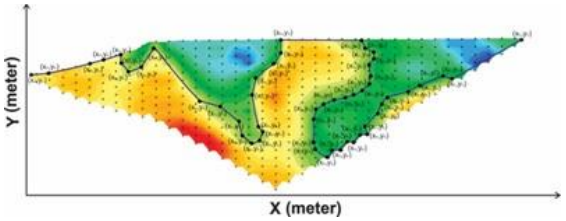

Fig.9 The data model is needed for modeling soil layers on slopes based on the results of TR data

For modeling the soil on a slope, an algorithm almost like the slope geometry algorithm is used, which is to detect the black lines, because from each soil layer in the geoelectric test results one may choose a color gradation display with a black line as the separating lines. Then, the following algorithms are used:

1. Sampling data points representing the shapes of soil layers is done manually by using the click tool so that the points (x, y) of the click points can be known. The sampling method is deliberately chosen so that the determination of soil stratigraphy can be adjusted to the soil drill data.
2. Inputting the click points (x, y) into Equations (28) and (29) below:

$$\text{x subsoil} = [x0 \quad x1 \quad x2 \quad x3 \quad x4 \quad x5 \quad x6 \quad x7] \tag{28}$$

$$y\,\text{subsoil} = [y0 \quad y1 \quad y2 \quad y3 \quad y4 \quad y5 \quad y6 \quad y7] \tag{29}$$

3. after obtaining the $x_{subsoil}$ and $y_{subsoil}$ matrices, the matrix results can be plotted on an (x-y) curve with slope geometry data as in Figure 10.

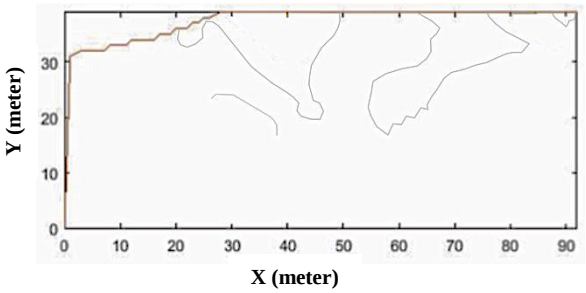

Fig.10 Result of soil stratigraphy determination

3.3 Model 3, Determination of Crack Positions

In determining areas of cracks, Tomographic Resistivity, TR, and Induced Polarization, IP, data are needed as shown in Figures 1 and 2. Both of those data will then be subjected into intersection process. Visualization of the intersection process is shown in Figure 11.

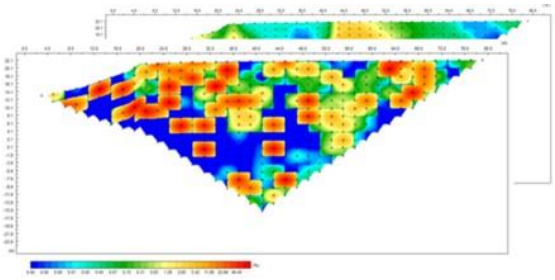

Fig.11 The intersection process in areas of blue colors in TR and IP images

The process to define the algorithms to retrieve cracks data is shown in the flowchart in Figure 12.

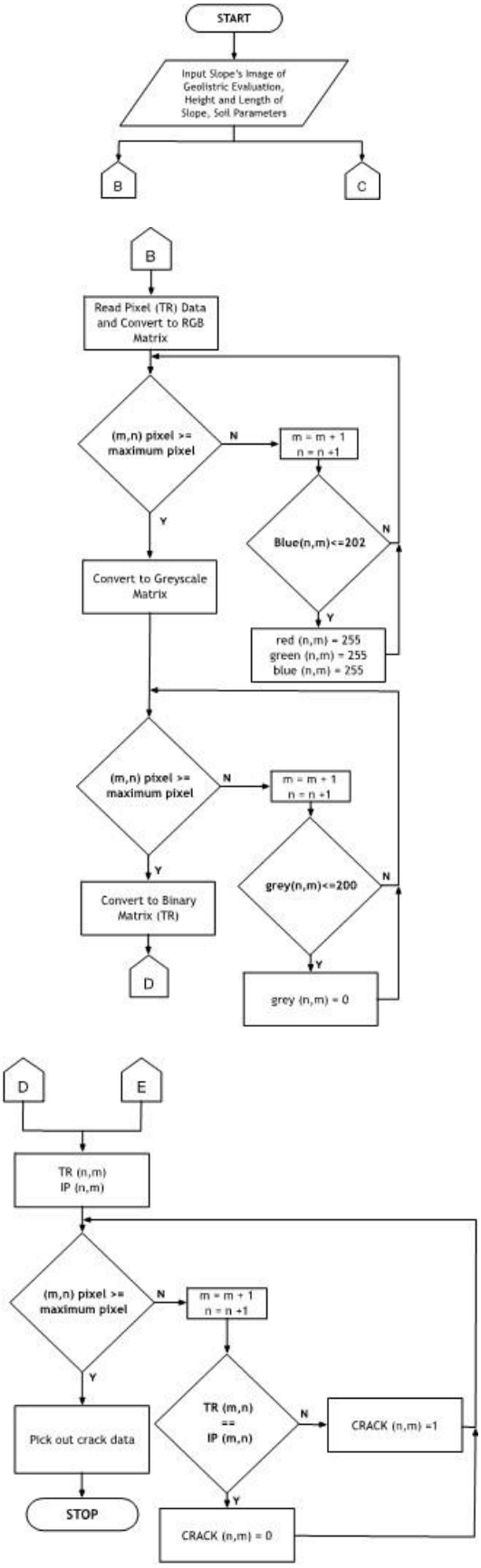

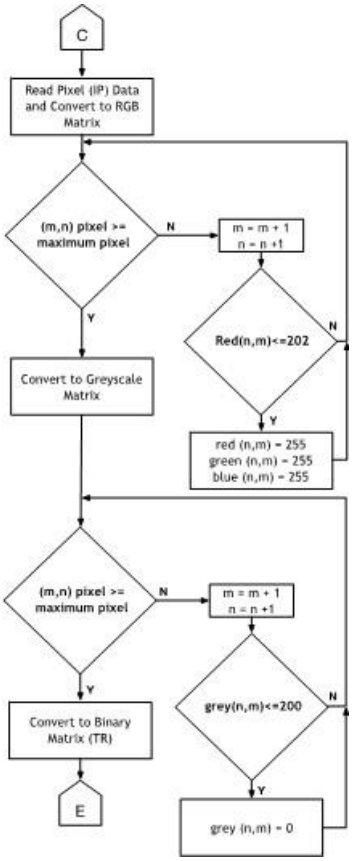

Fig. 12 Flowchart for detecting the TR and IP cracks data from geoelectric test results

Steps to read the TR data:

1. Inputting image data from geoelectric test results (Figure 1);
2. Interpreting the image into three matrices (RGB);
3. Color detection for blue intensity in the image for each pixel to distinguish blue color from other colors, so that the intensity of blue ≥ 202 is given. To determine that the color is blue, the following equation is used:

   if *blue (n,m)* ≤ 202 (bluish intensity)
   therefore
   red (n,m), green(n,m), blue(n,m) = 255 (30)
   The results of executing Equation 30 can be seen in Figure 13. From Figure 13, it is shown that the selected zone is exclusively blue, therefore it means those areas have a relatively high-water content.
4. Conversion of RGB into greyscale form.
5. Detection of the intensity of the darkest grey color on the image for each pixel that function to distinguish light gray with dark gray, sometimes even closer to black. It aims to take a high-intensity grey taken as grey ≥ 200 using the following equation:

   if *grey(n,m)* ≤ 200 (greyish intensity)
   therefore
   grey(n,m) = 0 (31)

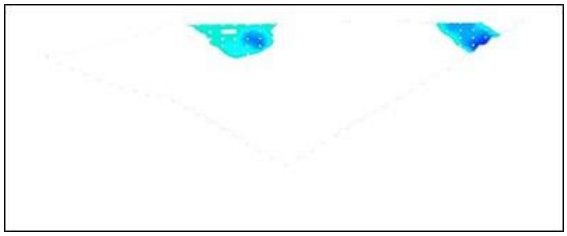

Fig. 13 The results of the image data after the stage of blue color intensity selection

6. Conversion from the grey matrices into the form of binary matrices, the final result is shown in Figure 14.

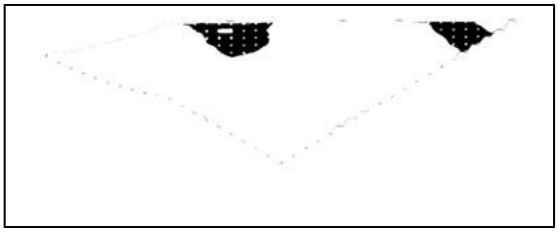

Fig. 14 Final result of the image data of blue color selection

Steps to read the IP data:

1. Inputting image data from geoelectric test results for IP data (Figure 2);
2. Interpreting the image into the three matrices (RGB);
3. Detecting the red intensity in the image for each pixel that functions to distinguish the red from other colors, so that the highest red color intensity ≥ 202 is taken using the following equation:

   if *red (n,m)* ≤ 202 (reddish intensity)
   therefore
   red (n,m), green(n,m), blue(n,m) = 255 (32)
   The results of the execution of the above equation can be seen in Figure 15.
4. Conversion of RGB into greyscale form.
5. Detection of the intensity of the darkest grey color on the image for each pixel that function to distinguish light gray with dark gray, sometimes even closer to black. It aims to take a high-intensity blue taken as grey ≥ 200 using the following equation:

   if *grey(n,m)* ≤ 200 (greyish intensity)
   therefore
   grey(n,m) = 0 (33)

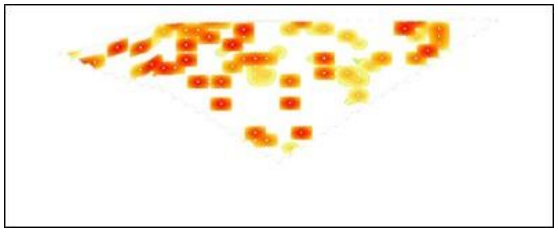

Fig. 15 The results of the image data after the stage of reddish color selection

6. Conversion grey matrices into binary matrices and the result can be shown in Figure 16.

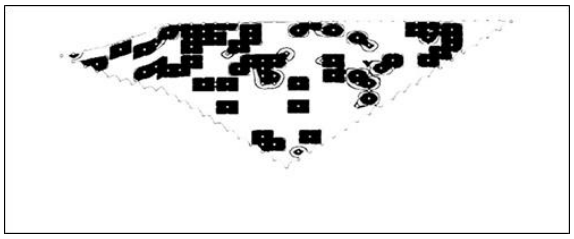

Fig. 16. The final result of the image data of red color detection

Integration of blue colors from TR and red colors from IP data to find the position of cracks is done by the following methods. Visualization of the intersection process is shown in Figure 17. The results of cracks are the results of the intersection of the area between TR and IP.

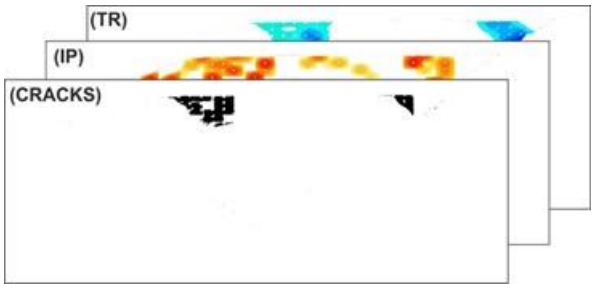

Fig. 17. Visualization of the intersection process and the result of the detected areas of cracks

1. The cracks detection requirements are applied as shown in Equation (34) thus the results of the image of the crack are shown in Figure 18.

Crack zone = intersection of the area between TR and IP. (34)

2. Sampling the area of cracks in the form of matrix equations is done manually with a picker tool that is already available on the program. Thus, when someone clicks on a point, a coordinate point (x, y) will show, and the complete data can be entered into the cracks area Equations (35)-(38).

Line 1

$$\mathbf{x\,c} = [\boldsymbol{x0}\ \ \boldsymbol{x1}\ \ \boldsymbol{x2}\ \ \boldsymbol{x3}\ \ \boldsymbol{x4}\ \ \boldsymbol{x5}\ \ \boldsymbol{x6}\ \ \boldsymbol{x7}] \quad (35)$$

$$\boldsymbol{y}\,\mathbf{c} = [\boldsymbol{y0}\ \ \boldsymbol{y1}\ \ \boldsymbol{y2}\ \ \boldsymbol{y3}\ \ \boldsymbol{y4}\ \ \boldsymbol{y5}\ \ \boldsymbol{y6}\ \ \boldsymbol{y7}] \quad (36)$$

Line 2

$$\mathbf{x\,c} = [\boldsymbol{x0}\ \ \boldsymbol{x1}\ \ \boldsymbol{x2}\ \ \boldsymbol{x3}\ \ \boldsymbol{x4}\ \ \boldsymbol{x5}\ \ \boldsymbol{x6}\ \ \boldsymbol{x7}] \quad (37)$$

$$\boldsymbol{y}\,\mathbf{c} = [\boldsymbol{y0}\ \ \boldsymbol{y1}\ \ \boldsymbol{y2}\ \ \boldsymbol{y3}\ \ \boldsymbol{y4}\ \ \boldsymbol{y5}\ \ \boldsymbol{y6}\ \ \boldsymbol{y7}] \quad (38)$$

Furthermore, the equation data for Line 1 and Line 2 are obtained to draw the crack areas. The data can be plotted so that visualization of the crack area can be established. The data above are then processed using algorithms and image processing techniques described previously so that finally the results of the image procession from the program can be drawn as in Figure 19.

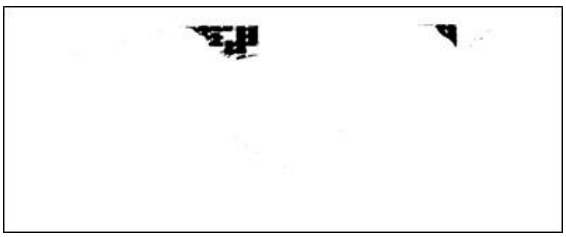

Fig. 18 Detected areas of cracks

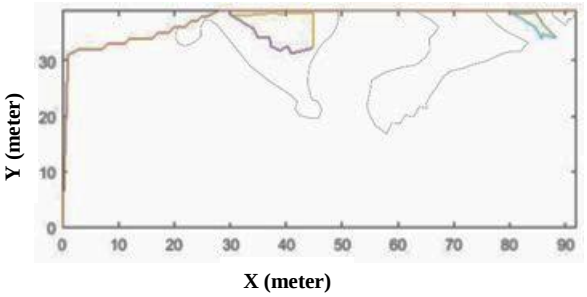

Fig. 19 The outcome of the program based on field data

From the results of image processing above, the accuracy and superiority of using the digital image processing techniques in this study can be described as follows:

1. The real size of the object of Figure 16 is 120 × 40 meters and the image has a pixel size of 2073 × 691 pixels. Therefore, the accuracy is 120m/2073 px, or = 0.0578 m/pixel, or equals to 5.78 cm/pixel. With this method, the geometry models, soil layers, and cracks can be determined in higher accuracy. This method can also be used to give more detailed modeling with accuracy reaching 5.78 cm from the results of the test images shown in Figure 19.
2. The accuracy level of slope data retrieval is higher because data retrieval is done with a scale according to the size of the slope. Hence, this method produces results of the slope geometry

modeling with proportional size and in accordance with the size of the results of geoelectric test data.
3. The existence of digital image processing techniques in research can also be used to detect the unevenness of a slope model, such as those given in Figure 19.
4. Cracks detection can be done easily considering the conditions to get the cracked areas by super-positioning the blue TR area and red IP area. This, of course, is very difficult if done without using the program and technique that is carried out in this study.
5. In the previous method, the digital data of the slope cross section is obtained by drawing again the shape of the embankments manually, according to their visual coordinates. This process has to be done at every cross section needed. However, when many analyses have to be performed on many cross sections in a 3-dimensional slope, the current manual process becomes cumbersome. The method offered in this study is automatical and digital so that the process of retrieving data is much faster.

4. CONCLUSION

Based on the results of the research that has been described above, the following conclusion is obtained:

1. Determining the slope geometry, soil stratigraphy, and cracks positions can be done faster and accurate by using digital image technology.
2. This digital image method can be detected up to 5.78 cm/pixel accuracy. Therefore, the greater the pixel size of the geoelectric test results, the higher the accuracy will be obtained. Accordingly, the more detailed and accurate geometry, layer, slope and slope modeling results could also be obtained.
3. The bigger the pixel size of the slope image processed, the accuracy level of the outcomes of the program will be higher. This method can also detect uneven slope geometries such as mounds or even wallows on any slope.
4. Detection of geometry and slope layer using black lines found in the geometry and slope layers. Thus, the coordinates of the geometry and the slope layer can be determined.
5. This digital image method can detect blue areas on TR and red areas on IP automatically. It can also do super-positioning the two areas so that the areas of cracks are obtained. This method will certainly be very difficult if not done using the digital image processing techniques as discussed in this study. Without this method, determination of the value of accuracy, scaling ratio, and color detection from the geoelectric test results data will be rather difficult and cumbersome.

The process of reading geoelectric data is done through computational techniques so that the geoelectric test data can be calculated quickly and accurately. This method can also process slope data while simultaneously calculating the value of the slope stability in a short period of time. As a result, the slope stability analysis can be done faster and more accurately.

5. ACKNOWLEDGMENTS

This paper was made to happen by the Hibah Penelitian Disertasi Doktor (Grant for Doctorate Dissertation) from the Directorate General for Research and Development, Ministry of Research and Higher Education, Republic of Indonesia, 2019. The authors wish to express their gratitude for the supports that were given to this work.

6. REFERENCES

[1] Mochtar I. B., "*Cara Baru Memandang Konsep Stabilitas Lereng Berdasarkan Kenyataan di Lapangan"* [New Method of Comprehending the Concept of Slope Stability Based on Field Evidences], Seminar Nasional Geoteknik Himpunan Ahli Teknik Tanah Indonesia (HATTI), Kalimantan Selatan, 2011, pp. 1-9.

[2] Mochtar I. B., "Kenyataan Lapangan sebagai Dasar untuk Usulan Konsep Baru tentang Analisa Kuat Geser Tanah dan Kestabilan Lereng" [Field Evidences as the Basis for A Proposed New Concept of Soil Strength and Slope Stability], Annual Meeting of Indonesian Society of Geotechnical Engineering (PIT HATTI), 2012, pp. 67-72.

[3] Mochtar I. B. and Hutagamissufadal , "Cracks in Soils and Their Implication for Geotechnical Engineering," 20th Annual National Conference on Geotechnical Engineering, 2016, pp. 1-6.

[4] Hutagamissufardal, Mochtar I. B., and Mochtar N. E., The Effect of Cracks Propagation on Cohesion and Internal Friction Angle for High Plasticity Clay, International Journal of Applied Engineering Research, Vol. 13, No.5, 2018, pp. 2504-2507.

[5] Hutagamissufardal, Mochtar I. B., and Mochtar N. E., The Effect of Soil Cracks on Cohesion and Internal Friction Angle at Landslide, Journal of Applied Environmental and Biological Sciences, Vol .8, No.3, 2018, pp. 1-

5.

[6] Alexsander S., Mochtar I. B., and Utama W., "The Measurements of Water Intrusion through Cracks Propagation Inside Slopes to Explain the Cause of Slope Failure—Case Study of Embankment in the Sanggu- Buntok Airport, Central Kalimantan, Indonesia", Electronic Journal of Geotechnical Engineering, Vol. 22, Issue 14, 2017, pp. 5347-5362.

[7] Alexsander S., Mochtar I. B., and Utama W., Field Validated Prediction of Latent Slope Failure Based on Cracked Soil Approach, Lowland Technology International, Vol. 20, Issue 3, 2018, pp. 245-258.

[8] Ikah N. P., Permanasari M., Fadli A., Gunawan H., and Lilik H., Determination of The Type of Soil Using 2D Geoelectric Method And Laboratory Analysis for Landslide Area Cililin West Java, Journal of Physics: Conf. Series 1127, 2019, pp. 1-6

[9] Oladunjoye M.A., Adefehinti A., and Ganiyu K.A.O., Geophysical appraisal of groundwater potential in the crystalline rock of Kishi area, Southwestern Nigeria, Journal of African Earth Sciences, Vol.11, 2018, pp. 1-26

[10] Shailaja G., Gupta G., Suneetha N., and Laxminarayana M., Assessment of aquifer zones and its protection via second-order geoelectric indices in parts of the drought-prone region of Deccan Volcanic Province, Maharashtra, India, Journal of Earth System Science, 128:78, 2019, pp.1-18

[11] Scott I. and Emily P., Preferential Groundwater Seepage in Karst Terrane Inferred from Geoelectric Measurements, Near Surface Geophysics, 2019, pp. 1-21

[12] Supriyadi, Agus S., Nurul P., Bowo E. C., and Imroatus S., Assessment of validated geoelectrical resistivity methods to reconstruct, Journal of Physics: Conference Series 1153, 2019, pp. 1-7

[13] Amalia D., Mochtar I. B., and Mochtar, N. E. "*Penerapan Konsep Baru Cracked Soils Pada Penanggulangan Kelongsoran Lereng"* [Application of the New Concept of Cracked Soils on Slope Eradication Management], Industrial Research Workshop and National Seminar, Vol. 9, 2017. pp. 50-62.

[14] PM. N and Chezian R. M., "Various Color Spaces and Color Space Conversion Algorithms", Journal of Global Research in Computer Science, Vol. 4, No.1, 2013, pp. 44-48.

[15] Mathworks, Matrix Laboratory (MATLAB), Massachusetts: Mathworks, 2014.